



## Research Paper

# Upregulation of pulmonary tissue factor, loss of thrombomodulin and immunothrombosis in SARS-CoV-2 infection

Ivo M.B. Francischetti<sup>a,\*</sup>, Kevin Toomer<sup>a</sup>, Yifan Zhang<sup>b</sup>, Jayesh Jani<sup>a</sup>, Zishan Siddiqui<sup>c</sup>, Daniel J. Brotman<sup>c</sup>, Jody E. Hooper<sup>a</sup>, Thomas S. Kickler<sup>a</sup>

<sup>a</sup> Department of Pathology, Johns Hopkins University School of Medicine, Baltimore, MD, United States

<sup>b</sup> Department of Biostatistics, Johns Hopkins University Bloomberg School of Public Health, Baltimore, MD, United States

<sup>c</sup> Department of Medicine, Johns Hopkins University School of Medicine, Baltimore, MD, United States

## ARTICLE INFO

## Article History:

Received 19 April 2021

Revised 15 July 2021

Accepted 20 July 2021

Available online xxx

## Keywords:

Thrombosis

Hemostasis

Coagulation

Ixolaris

## ABSTRACT

**Background:** SARS-CoV-2 infection is associated with thrombotic and microvascular complications. The cause of coagulopathy in the disease is incompletely understood.

**Methods:** A single-center cross-sectional study including 66 adult COVID-19 patients (40 moderate, 26 severe disease), and 9 controls, performed between 04/2020 and 10/2020. Markers of coagulation, endothelial cell function [angiopoietin-1,-2, P-selectin, von Willebrand Factor Antigen (WF:Ag), von Willebrand Factor Ristocetin Cofactor, ADAMTS13, thrombomodulin, soluble Endothelial cell Protein C Receptor (sEPCR), Tissue Factor Pathway Inhibitor], neutrophil activation (elastase, citrullinated histones) and fibrinolysis (tissue-type plasminogen activator, plasminogen activator inhibitor-1) were evaluated using ELISA. Tissue Factor (TF) was estimated by antithrombin-FVIIa complex (AT/FVIIa) and microparticles-TF (MP-TF). We correlated each marker and determined its association with severity. Expression of pulmonary TF, thrombomodulin and EPCR was determined by immunohistochemistry in 9 autopsies.

**Findings:** Comorbidities were frequent in both groups, with older age associated with severe disease. All patients were on prophylactic anticoagulants. Three patients (4.5%) developed pulmonary embolism. Mortality was 7.5%. Patients presented with mild alterations in the coagulogram (compensated state). Biomarkers of endothelial cell, neutrophil activation and fibrinolysis were elevated in severe vs moderate disease; AT/FVIIa and MP-TF levels were higher in severe patients. Logistic regression revealed an association of D-dimers, angiopoietin-1, vWF:Ag, thrombomodulin, white blood cells, absolute neutrophil count (ANC) and hemoglobin levels with severity, with ANC and vWF:Ag identified as independent factors. Notably, postmortem specimens demonstrated epithelial expression of TF in the lung of fatal COVID-19 cases with loss of thrombomodulin staining, implying in a shift towards a procoagulant state.

**Interpretation:** Coagulation dysregulation has multifactorial etiology in SARS-Cov-2 infection. Upregulation of pulmonary TF with loss of thrombomodulin emerge as a potential link to immunothrombosis, and therapeutic targets in the disease.

**Funding:** John Hopkins University School of Medicine.

© 2021 The Author(s). Published by Elsevier Ltd. This is an open access article under the CC BY-NC-ND license (<http://creativecommons.org/licenses/by-nc-nd/4.0/>)

## 1. Introduction

The pandemic caused by severe acute respiratory syndrome coronavirus 2 (SARS-CoV-2) resulted in high morbidity and mortality with an enormous impact on public health [1]. Infection by the virus produces a systemic inflammatory response associated with respiratory failure, pneumonia and multiorgan dysfunction [2,3]. Most patients also develop a coagulopathy characterized by elevated D-dimers [4–9]. The coagulopathy promotes a prothrombotic state, with high prevalence of venous thromboembolism and some reports of arterial thrombosis [4–9]. Different mechanisms have been proposed to explain the coagulation dysregulation. Accordingly, an

**Abbreviations:** vWF, von Willebrand Factor; vWF:Ag, von Willebrand Factor Antigen; vWF:RCo, von Willebrand Factor Ristocetin Cofactor; ADAMTS13, a disintegrin and metalloproteinase with a thrombospondin type 1 motif, member 13; sEPCR, soluble Endothelial cell Protein C Receptor; TFPI, Tissue Factor Pathway Inhibitor; t-PA, tissue-type plasminogen activator; PAI-1, plasminogen activator inhibitor-1; TF, Tissue Factor; AT/FVIIa, antithrombin-FVIIa complex; MP-TF, Microparticles-Tissue Factor; Hb, hemoglobin; ANC, absolute neutrophil count; AMC, absolute monocyte count; ALC, absolute lymphocyte count; WBC, white blood cells; ELISA, enzyme-linked immunosorbent assay; PAR, protease-activated receptor; ICU, intensive care unit; LMWH, low molecular weight heparin; ALL, Acute Lung Injury

\* Corresponding author.

E-mail address: [lfranci3@jhmi.edu](mailto:lfranci3@jhmi.edu) (I.M.B. Francischetti).

<https://doi.org/10.1016/j.eclinm.2021.101069>

2589-5370/© 2021 The Author(s). Published by Elsevier Ltd. This is an open access article under the CC BY-NC-ND license (<http://creativecommons.org/licenses/by-nc-nd/4.0/>)

## Research in context

### Evidence before this study

The mechanisms of coagulopathy in SARS-CoV-2 is incompletely understood, with endothelial cells and neutrophils playing a significant role in this process. Whether Tissue Factor (TF), the clotting initiator play a role in coagulation dysregulation remains elusive, as well as pulmonary expression of thrombomodulin and Endothelial Cell Protein C Receptor (EPCR).

### Added value of this study

Antithrombin/FVIIa complex, a marker of *in vivo* TF expression and TF-containing microparticles are significantly elevated in plasma of patients with severe COVID-19 infection. Notably, upregulation of TF in the alveolar epithelial cells of fatal SARS-CoV-2 was demonstrated in our autopsy cases, a finding supported by recent transcriptional analysis showing upregulation of TF mRNA in the alveolar epithelial cells. We also show loss of thrombomodulin in lung capillaries, consistent with down regulation of its corresponding transcript, also recently reported.

### Implications of all the available evidence

These results imply in a shift towards a procoagulant state, with the lung as a major source of procoagulant stimulus in the disease. Upregulation of pulmonary TF with loss of thrombomodulin emerge as a novel link to immunothrombosis. Together with components of the Virchow's triad (hypercoagulability, endothelial injury, stasis), it helps to explain the high incidence of thrombosis in these patients.

complex mechanism of hemostatic dysregulation takes place, with the lung playing a major role in this process by providing pro-coagulant stimuli to fuel the coagulation and inflammation cycle, consistently reported in the disease.

### 1.1. Material and methods

#### 1.1.1. Study design and participants

Cross-sectional study of 66 adult ( $\geq 18$  years) patients with moderate disease (referred as "moderate disease group",  $n=40$ ) and severe or critical disease (referred as "severe disease group",  $n=26$ ), based on WHO guidelines [42], with clinical and/or radiologic indications for hospitalization at the Johns Hopkins Hospital (period 04/20–10/20). About 40% of patients in the severe group required mechanical ventilation consistent with critical disease. All patients had a confirmed diagnosis of COVID-19 by polymerase-chain reaction (PCR) assays on nasopharyngeal swab samples. We included additional 9 individuals negative for COVID-19 with no significant pathology, who served as controls. Patient characteristics including age, sex, major comorbidities, laboratory and imaging results, and treatments were recorded in Electronic Medical Records (EMRs), with 2 authors (I.F., K.T.) having access to data. All experiments using human material were performed in accordance with Institutional guidelines (IRB00257218) and the agreement of the Ethical Committee of the Johns Hospital University School of Medicine. The Institutional Review Board approved this study and waived the need for consent.

#### 1.1.2. Procedures

The median and interquartile range [IQR] for all collections was 1 day [0–2.25] after admission. The time of collection was 9.01 am [5.2 am–15.78 pm]. Blood samples were collected into Vacutainer tubes (BD, Franklin Lakes, New Jersey) containing sodium citrate (3.2%) and were centrifuged once at  $2000 \times g$  for 10 min at room temperature to obtain platelet-poor plasma. The supernatant was collected and centrifuged again as above. Plasma was stored at  $-80^\circ\text{C}$  until the time of assay.

#### 1.1.3. ELISA and other reagents

All hematologic parameters, PT, aPTT, D-dimer and fibrinogen, von Willebrand Factor antigen (vWF:Ag), von Willebrand activity (vWF:RCo) were performed at our Institution's clinical laboratory Siemens CS-5100 (Siemens; Malvern, PA, USA) with manufacturer's reagents and controls per laboratory protocol. DUOSet ELISA (enzyme-linked immunosorbent assay) was performed for human angiopoietin-1 (DY623), angiopoietin-2 (DY923), elastase (DY9167), P-selectin/CD62P (DY137), soluble endothelial protein C receptor (sEPCR, DY2245), plasminogen activation inhibitor-1 (PAI-1, DY1786), Tissue Factor Pathway Inhibitor (TFPI, DY2974), thrombomodulin (DY3947), tissue-type plasminogen activator (t-PA, DY7449) (R&D, Minneapolis, MN), Asserachrom Antithrombin-Factor VIIa (AT/FVIIa) complex was from Stago (Asnières sur Seine, France). Zymogen Microparticle-Tissue Factor (MP-TF) was purchased from Hyphen Biomed/Aniara Diagnostica (West Chester, OH). ADAMTS13 activity was determined with Immucor enzyme assay kit (Peachtree, GA). Enzygnost F1 + 2 (monoclonal) was obtained from Siemens. Citrullinated Histone H3 ELISA was from Cayman Chemical (Ann Arbor, MI). ELISA was performed according to the manufacturer's instructions, using a Synergy HTX Multi-mode Microplate Reader, interfaced with Gen5 2.09 Software (BioTek Instruments, VT).

#### 1.1.4. Calibrated automated thrombography (CAT)

Thrombinoscope assay was performed on a microtiter plate using the Calibrated Automated Thrombogram assay (Thrombinoscope BV, Maastricht, the Netherlands), as described [43]. The CAT reagents contain PPP-reagent (a mixture of 4 pmol/L phospholipids and 5 pmol/L Tissue Factor), thrombin calibrator and FluCa-kit (a mixture

endotheliopathy has been described as a hallmark of the disease and supported by the identification of viral inclusions in endothelial cells, apoptosis, and an increase in plasma or serum biomarkers of endothelial cell activation [10–15].

More recently, the innate immune response and immunothrombosis have been implicated in disease pathogenesis [16–20]. Elevated Neutrophil Extracellular Traps (NETs) were found in plasma of infected patients, corroborating the view that neutrophils play an active role in disease coagulopathy [21–27]. Platelet-monocytes aggregates, complement cascade and thrombotic microangiopathy have also been identified as critical components of the disease [28–30]. In addition, numerous autopsy studies revealed endothelial cell injury, complement activation, with detection of NETs, fibrin and platelet thrombi in vascular beds of the lung in SARS-Cov-2 (COVID-19) [31–35]. More recently, scRNA-seq analysis showed increased expression of Tissue Factor (TF), the clotting initiator [36,37] in epithelial cells from the bronchoalveolar lavage (BAL) from patients with COVID-19, but much lower expression in other cell types [38]. Whether these changes translate in upregulation of TF protein in the lung, and its cellular distribution remained elusive thus far. Another recent study reported a reduction in pulmonary transcriptional levels of thrombomodulin [39], a major endothelial cell anticoagulant [40,41]. Likewise, it is unknown whether thrombomodulin expression in the endothelial cell of small vessels, where it normally resides [41] is downregulated in the lung of patients who succumbed from the disease.

The primary objective of our study was to concomitantly evaluate biomarkers of cellular activation and hemostatic dysregulation in COVID-19 patients. The secondary goal was to investigate an association of several biomarkers with moderate or severe disease. The third objective was to study the expression of hemostatic components in the lungs from patients with COVID-19 ALL. Our findings show that a

of Fluo-Substrate and Fluo-Buffer). Plasma (80  $\mu$ L) was incubated with Ixolaris (0–20 nM) for 15 min, followed by addition of thrombin calibrator (20  $\mu$ L) in one set of wells, and PPP-Reagent (20  $\mu$ L) in another set of wells to activate coagulation, both for 10 min. Thrombin generation was started with the FluCa-kit. Several parameters can be derived from the thrombin generation curve, including endogenous thrombin potential (nmol/L/min; the area under the thrombin generation curve), lag time (the time from thrombin generation to reach one-sixth of the peak concentration), peak thrombin (nmol/L; the maximal height of the thrombogram), and the tpeak (min; time to peak thrombin generation). All samples were run in triplicate. Ixolaris, a specific inhibitor of TF/VIIa, was expressed and purified as described [44].

#### 1.1.5. Disseminated intravascular coagulation (DIC) score determination

The International Society of Thrombosis and Hemostasis (ISTH) DIC score is calculated using platelet count ( $\geq 100,000 = 0$ ;  $50,000-99,999 = 1$ ;  $< 50,000 = 2$ ), fibrinogen level ( $\geq 100 \text{ mg/dL} = 0$ ;  $< 100 \text{ mg/dL} = 1$ ), prothrombin time prolongation above upper limit of normal (ULN) ( $< 3 \text{ s} = 0$ ,  $3-6 \text{ s} = 1$ ,  $> 6 \text{ s} = 2$ ), and D-dimer ( $< 2 \text{ times ULN} = 0$ ,  $2-4 \text{ times ULN} = 2$ ,  $> 4 \text{ times ULN} = 3$ ) [45].

#### 1.1.6. Autopsy

All autopsies were performed by the Autopsy Service at the Johns Hopkins Hospital, and described in detail elsewhere [46].

#### 1.1.7. Immunohistochemistry (IHC) studies

Immunostaining was carried out at the Oncology Tissue Services Core of Johns Hopkins University School of Medicine. Immunolabeling for all antigens was performed on formalin-fixed, paraffin embedded sections on a Ventana Discovery Ultra autostainer (Roche Diagnostics). Following dewaxing and rehydration on board, epitope retrieval was performed using Ventana Ultra CC1 buffer (Roche Diagnostics) at 96 °C for 64 min. Primary antibodies rabbit polyclonal anti-TF (1:400; PA-27,278; Thermofisher), rabbit polyclonal anti-thrombomodulin (1:1000; PA5-81,618, Thermofisher) and mouse monoclonal anti-endothelial cell protein C receptor (EPCR, PROCR) (1:800; UMAB200, Origine) were applied at 36 °C for 60 min. Primary antibodies were detected using an anti-rabbit or anti-mouse HQ detection system. This step was followed by Chromomap DAB IHC detection kit (Roche Diagnostics), counterstaining with Mayer's hematoxylin, dehydration and mounting. CD61 was employed for detection of platelet thrombi, CD68 for macrophages and AE1/AE3 (cytokeratin cocktail) for epithelial cells using automated staining. For each case, one IHC slide was independently semi-quantitatively scored by 2 pathologists (I.F., J.H.) with excellent inter-observer agreement, as follows: rare or absent (0),  $\leq 10\%$  (1+), 11–25% (2+), 26–50% (3+),  $> 51\%$  (4+). Mann-Whitney *U* test was employed for statistical analysis.

#### 1.1.8. Statistical analysis

Descriptive statistics are expressed as percentages, mean  $\pm$  standard deviation (SD)/standard error of mean (SEM), or median and inter-quartile range [IQR]. Categorical data were tested using Fisher's exact test (two-tailed). Normal distribution was verified using the D'Agostino-Pearson test. For variables with non-parametric distributions, the Mann-Whitney *U* test (2 groups), or Kruskal-Wallis test (3 or more groups) followed by Dunn pairwise post hoc comparisons were employed. For markers containing reference lab values, and 2 subgroups, Mann-Whitney *U* test was employed. Spearman rank coefficient correlation tested the association between quantitative variables, and generation of heatmaps (GraphPad Prism version 8.4.2). A *p* value of  $< 0.05$  was considered significant. Univariate logistic and multivariate logistic regression models were constructed using R Version 3.6.2 to assess predictors of case severity. All variables with *p* values  $< 0.05$  from the univariate analysis and with fewer

than 5 missing data points were selected for multivariate analysis, and lasso regularization was applied to arrive at the final multivariate model.

#### 1.1.9. Role of funding

The funding source did not have any role in study design and/or data analysis or interpretation.

### 1.2. Results

#### 1.2.1. Demographics

Sixty six adult patients (40 with moderate and 26 with severe disease) with PCR-confirmed SAR-COV-2 were included in our cohort. Nine healthy individuals were included as controls (Table 1). Age was the only variable to show a statistically significant difference between moderate and severe cases (47 yo vs 66 yo,  $p < 0.001$ ), while sex, body mass index (BMI) and comorbidities did not differ. The most common comorbidities combined for both groups were obesity (75%), hypertension (35%), diabetes (30%) and asthma (20%). Other less common comorbidities included history of venous thrombosis, chronic kidney disease and history of malignancy. All patients were on prophylactic dose anticoagulation according to guidelines recommendations for standard intensity or high-intensity anticoagulation based on patient's risk profile [47]. Approximately 80% of them were on low molecular weight heparin (LMWH, enoxaparin), and few others on unfractionated heparin (10%), warfarin or direct oral anti-coagulant (DOACs) (6.0%). Three patients (7.5%) in the moderate disease group or 4.5% of all patients, developed pulmonary embolism, with no deaths. In the severe disease group, 5 patients died (19%), corresponding to 7.5% of all patients. There was no thrombosis documented during hospitalization of severe patients.

#### 1.2.2. Routine biochemical and hematologic parameters

The following markers were elevated in the severe vs moderate disease group with the means  $\pm$  SEM or median and [IQR] for each variable indicated in Table 1. Numerous hematologic parameters differentiated both groups statistically including hemoglobin (Hb,  $p = 0.006$ ), white blood cell count (WBC,  $p < 0.0001$ ) and absolute neutrophil count (ANC,  $p < 0.0001$ ), but not absolute monocyte count (AMC) and lymphocyte counts (ALC). In addition, creatinine ( $p = 0.0007$ ), lactate dehydrogenase (LDH,  $p = 0.0001$ ), ferritin ( $p = 0.015$ ) and interleukin-6 (IL-6,  $p = 0.03$ ) were statistically significant between groups, in contrast to C-reactive protein (CRP). There was no statistical significance in these parameters ( $p > 0.05$ ) when moderate disease group was compared with control.

#### 1.2.3. Global coagulation parameters and sofa scores

Table 1 shows that PT, aPTT and fibrinogen did not differ between moderate and severe disease groups, while platelet count ( $p = 0.006$ ), D-dimers ( $p = 0.0001$ ) and Prothrombin fragment 1 + 2 (P1 + 2,  $p = 0.035$ ) were discriminatory. The DIC score, based on the ISTH criteria [45], was significantly higher in severe vs moderate disease group ( $p = 0.0003$ ), but averaged less than 5 in both groups. Among coagulation markers, only the aPTT ( $p = 0.02$ ) and P1 + 2 ( $p < 0.0001$ ) showed statistically significant difference between moderate disease and control groups. The SOFA score [48] at hospital or ICU admission was  $3.4 \pm 0.4$  with a maximum score was  $5.9 \pm 0.8$ . The SOFA score for each severe patient, time of intubation, associated infections, ventilation/respiratory support is presented in the Supplemental Table S1.

#### 1.2.4. Endotheliopathy

The COVID-19 infection has been associated with an endotheliopathy [10–15]. vWF is present in endothelial Weibel-Palade bodies and released upon cytokine stimulation as large multimers which are proteolytic processed by ADAMTS13, a metalloproteinase that cleaves ultra-large VWF multimers into smaller VWF forms [49].

**Table 1**  
Demographics, laboratory, anticoagulant use, clinical and outcome information for cohort cases.

	Control (n = 9)	Moderate (n = 40)	Severe (n = 26)	p value <sup>a</sup>
<b>Demographics</b>				
Sex, male	5 (55)	19 (47.5)	14 (53.8)	NS <sup>a</sup>
Age, years	47 [23–51]	47 [22–65.2]	66 [34–78]	0.0006 <sup>b</sup>
BMI, Kg/m <sup>2</sup>	26.6 [24.0–30.1]	29.84 [25.8–36.0]	30.5 [24.0–35.9]	NS <sup>b</sup>
Comorbidities	0 (0)	30 (75)	20 (77)	NS <sup>a</sup>
<b>Comorbidities</b>				
Obesity	–	33 (82.5)	17 (65)	NS <sup>a</sup>
Hypertension	–	12 (30)	11 (42)	NS <sup>a</sup>
Diabetes	–	10 (25)	10 (38)	NS <sup>a</sup>
Asthma	–	8 (20)	5 (19)	NS <sup>a</sup>
Coronary artery disease, MI, TIA, stroke	–	4 (10)	7 (27)	NS <sup>a</sup>
Venous thrombosis or pulmonary embolism	–	2 (5)	2 (7.5)	NS <sup>a</sup>
Chronic Kidney Disease	–	2 (5)	3 (11)	NS <sup>a</sup>
Active or past history of malignancy	–	4 (10)	3 (11)	NS <sup>a</sup>
<b>Routine Laboratory Tests</b>				
Hemoglobin (g/dl)	13.7 [12.6–14.2]	12.7 [11.5–14.0]	11.20 [9.8–12.9]	0.02 <sup>b</sup>
White blood cell (K/ $\mu$ l)	5.2 [4.7–9.7]	5.2 [4.2–7.1]	9.3 [6.7–11.5]	<0.0001 <sup>b</sup>
Absolute monocyte count (K/ $\mu$ l)	0.43 [0.3–0.5]	0.37 [0.3–0.5]	0.54 [0.3–0.6]	NS <sup>b</sup>
Absolute lymphocyte count (K/ $\mu$ l)	1.6 [1.2–1.8]	1.1 [0.83–1.7]	1.1 [0.7–1.5]	NS <sup>b</sup>
Absolute neutrophil count (K/ $\mu$ l)	3.0 [2.5–4.8]	3.6 [2.5–4.7]	7.3 [5.3–9.2]	<0.0001 <sup>b</sup>
C-reactive protein (mg/dl)	Ref. (0–4.9)	5.0 [2–9.3]	11.5 [2.2–21.3]	NS <sup>c</sup>
Plasma creatinine (mg/dl)	Ref. (0.6–1.3)	0.77 [0.6–0.95]	1 [0.8–1.2]	0.0007 <sup>c</sup>
Lactate dehydrogenase (U/L)	Ref. (84–197)	288.5 [258–1053]	623 [358–1053]	0.0001 <sup>c</sup>
Ferritin (ng/ml)	Ref. (13–150)	561 [202–892]	812 [516–1869]	0.015 <sup>c</sup>
Interleukin-6 (pg/ml)	Ref. (<10 pg/ml)	29.2 [16.6–52.69]	36.8 [24.8–126.5]	0.03 <sup>c</sup>
<b>Coagulation</b>				
PT (sec)	10.4 [10.4–11.3]	11.1 [10.8–11.4]	11.2 [10.8–11.7]	NS <sup>b</sup>
aPTT (sec)	28.8 [27.9–30.5]	32.4 [30.7–33.4]	29.5 [27.3–34.4]	NS <sup>b</sup>
Fibrinogen (mg/ml)	Ref. (170–422)	475.5 [409.3–543.3]	572.5 [428–687]	NS <sup>c</sup>
Platelets (K/ $\mu$ l)	232 [202–262]	188 [162–256]	271 [213–313]	0.006 <sup>b</sup>
D-dimers (mg/ml)	0.34 [0.20–0.4]	0.61 [0.36–0.93]	1.33 [0.84–3.3]	0.0001 <sup>b</sup>
Prothrombin 1 + 2 (pmol/l)	301.1 [249–440]	1908 [1051–3018]	1316 [687.3–1737]	0.035 <sup>b</sup>
DIC score	0	0.67 (0.17)	1.9 (0.25)	0.0003 <sup>b</sup>
<b>Anticoagulants</b>				
LMWH (enoxaparin)	–	33 (82.5)	21 (80.7)	NS <sup>a</sup>
Standard Heparin	–	4 (10)	3 (11.5)	NS <sup>a</sup>
Warfarin	–	1 (2.5)	0 (0)	NS <sup>a</sup>
Rivaroxaban or Apixaban	–	2 (5)	2 (7.6)	NS <sup>a</sup>
<b>Thrombosis (during hospitalization)</b>				
Venous Thrombosis	0	0	0	NS <sup>a</sup>
Pulmonary Embolism	0	3 (7.5)	0	NS <sup>a</sup>
Coronary artery disease, MI, TIA, stroke	0	0	0	NS <sup>a</sup>
<b>Hospital stay and Outcome</b>				
ICU stay	0	0	18 (69.2)	0.0001 <sup>a</sup>
Death	0	0	5 (19.2)	0.0074 <sup>a</sup>

Value reported as n (%), mean (SEM), or median [IQR].

<sup>a</sup> Fisher's exact test, two-tailed (categorical variable).

<sup>b</sup> Kruskal-Wallis test or.

<sup>c</sup> Mann-Whitney U test (continuous variables).

\* p values refer to comparison between mild and severe disease groups.

BMI, body mass index; LMWH, low-molecular weight heparin.

MI, myocardium infarction; TIA, transient ischemic attack; ICU intensive care unit.

NS, non-significant.

Excessive release of vWF, particularly high molecular weight forms, may cause microcirculatory dysfunction by spontaneous binding to platelets, leading to thrombotic microangiopathy. We determined vWF antigen levels (vWF:Ag) and vWF:Ristocetin cofactor activity (vWF:RCO) in all samples. vWF:Ag levels were statistically significantly higher in moderate and severe cases than in normal controls ( $p=0.0021$  and  $p < 0.0001$ , respectively), and also differentiated moderate vs severe disease groups ( $p=0.0014$ ) (Fig. 1A). Likewise, vWF cofactor activity (vWF:RCO) was significantly elevated in moderate and severe cases vs controls ( $p=0.026$  and  $<0.0001$ , respectively), and in severe vs moderate disease groups ( $p=0.0042$ ) (Fig. 1B). ADAMTS 13 activity, showed a trend towards lower levels in moderate and severe COVID-19 patients compared with control, but did not reach the conventional  $p < 0.05$  value of statistical significance (Fig. 1C).

Thrombomodulin (TM) is a cell surface-expressed glycoprotein, and critical cofactor for thrombin-mediated activation of protein

C (PC), amplified by the endothelial cell protein C receptor (EPCR). Activated PC (APC) is known for its natural anticoagulant properties by cleaving cofactors Factor Va and Factor VIIIa [41,50]. Upon cell activation, cleaved thrombomodulin can be detected in plasma. We noted much higher levels of soluble thrombomodulin in severely affected patients than healthy individuals ( $p=0.02$ ) (Fig. 1D). EPCR promotes generation of APC by the thrombin–thrombomodulin complex and promotes anti-inflammatory signals through protease-activated receptor 1 (PAR-1) [51]. We found statistically significant differences in sEPCR between moderate and severe disease groups compared to controls ( $p=0.015$  and  $p=0.04$ , respectively) (Fig. 1E). We also determined the levels of TFPI, a major anticoagulant of the extrinsic pathway. [36,37] Fig. 1F shows much higher levels of TFPI in moderate and severe COVID-19 patients vs controls ( $p=0.0002$  and  $p < 0.0001$ ), but no statistically significant difference was found between these 2 groups.

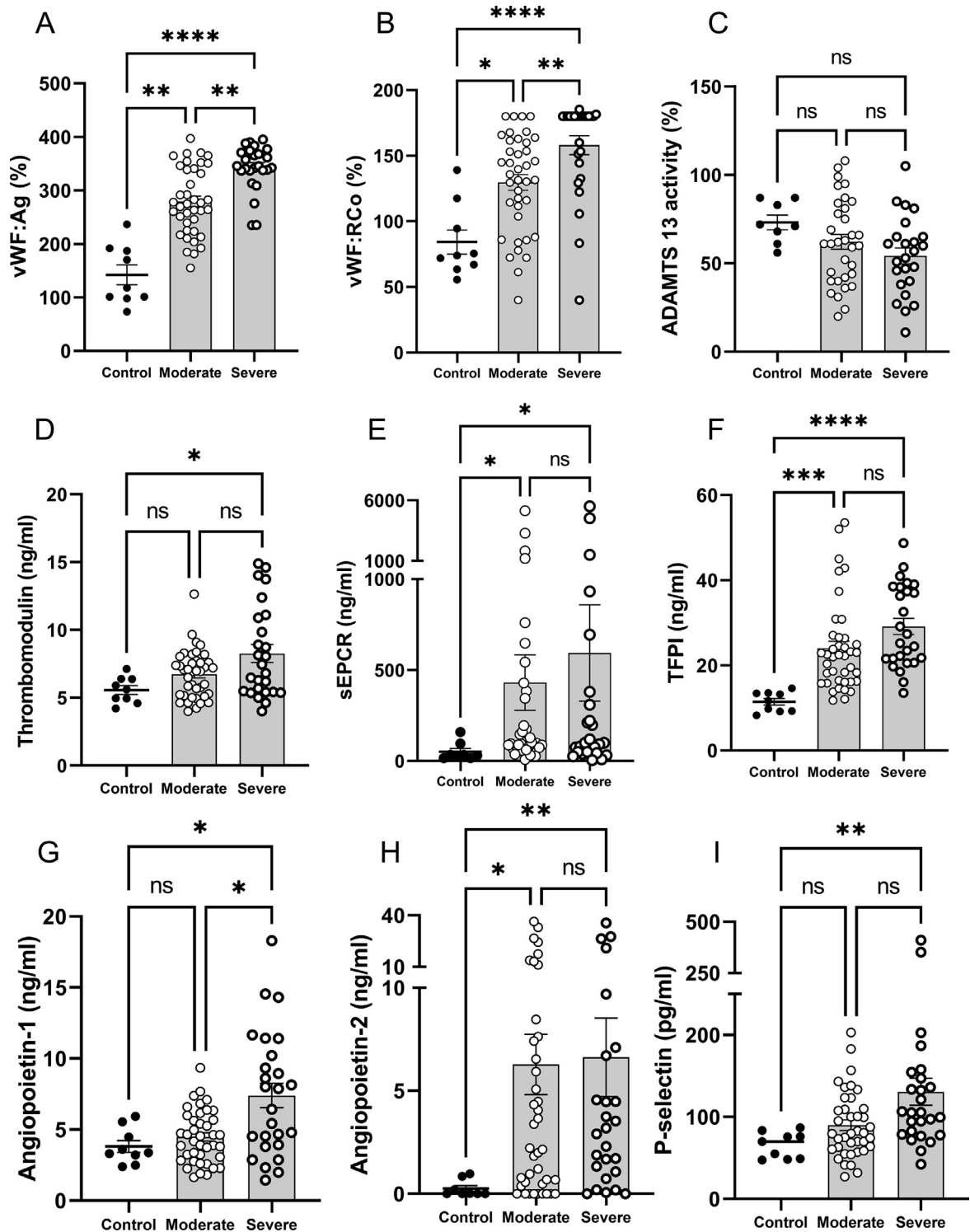


**Fig. 1.** Biomarkers of endothelial cell activation in SARS-CoV-2 infection and controls. (A) vWF:Ag, (B) vWF:RCo, (C) ADAMTS13, (D) thrombomodulin, (E) sEPCR, (F) TFPI, (G) Angiopoietin-1, (H) Angiopoietin-2 and (I) P-selectin plasma concentrations were determined by ELISA in healthy controls and COVID-19 patients. Each symbol correspond one patient. Shaded bars indicate the means, and the lines show the SEM. NS, non-significant; \* $p < 0.05$ ; \*\* $p < 0.01$ , \*\*\* $p < 0.001$ , \*\*\*\* $p < 0.0001$  (Kruskal-Wallis test, or Mann-Whitney  $U$  test).

Angiopoietins are endothelium-derived angiogenic factors with potent effects on the vascular endothelium. Endothelial damage associated with inflammation and hypoxia stimulates the exocytosis of endothelial Weibel-Palade bodies and the rapid release of angiopoietin-2. The binding of angiopoietin-2 to its tyrosine kinase (Tie-2) receptor is associated with impairment of vessel integrity, and it enhances endothelial inflammation, while angiopoietin-1 has an opposite effect [52]. Fig. 1G shows higher levels of Angiopoietin-1 in

severe vs moderate disease ( $p=0.02$ ) and severe vs control cases ( $p=0.03$ ), but not moderate cases vs controls ( $p > 0.99$ ). Angiopoietin-2 was elevated in moderate and severe cases vs control ( $p=0.01$  and  $p=0.007$ , respectively), but did not differentiate moderate vs severe diseases, with  $p > 0.99$  (Fig. 1H). P-selectin is released from endothelial cells and platelet  $\alpha$  granules upon activation. [50] Our cohort demonstrated elevated P-selectin levels in severe cases vs controls ( $p=0.045$ ), indicative of cellular activation (Fig. 1I).

### 1.2.5. Neutrophil activation and fibrinolysis

The innate immune response is induced by the formation of thrombi inside microvessels. This process, known as immunothrombosis is supported by immune cells and a substantial part of it is driven by neutrophils and neutrophil extracellular traps (NETs) [16–27]. NETs triggers the contact pathway of coagulation by interacting with FXII, and activate platelets and endothelial cells through histones. In addition, NETs-associated neutrophil elastase cleaves TFPI, resulting in inactivation of endogenous anti-coagulants and propagation of coagulation. Plasma levels of citrullinated histones are employed as a marker of NETs [19]. We noted higher levels of citrullinated histones in moderate and severe patients than in controls ( $p=0.026$  and  $p=0.04$ ), but not between these 2 groups, with  $p > 0.99$  (Fig. 2A). Elastase is a

pro-inflammatory and pro-coagulant enzyme released by neutrophils [16–19]. We found statistically significant differences in elastase between moderate and severe groups compared to health individuals ( $p=0.02$  and  $p < 0.0001$ , respectively), and between moderate and severe disease ( $p=0.001$ ) (Fig. 2B). We also investigated changes in fibrinolysis.  $t$ -PA, an enzyme that activates the zymogen plasminogen into the enzyme plasmin, degrades fibrin clots and is inhibited by PAI-1 [50].  $t$ -PA levels trended higher in moderate disease group compared to controls ( $p=0.16$ ), and reached statistical significance for severe patients vs controls ( $p=0.002$ ) and also for moderate vs severe disease ( $p=0.024$ ) (Fig. 2C). PAI-1 levels were much higher in moderate and severe patients compared to controls ( $p=0.003$  and  $p=0.004$ , respectively) (Fig. 2D).

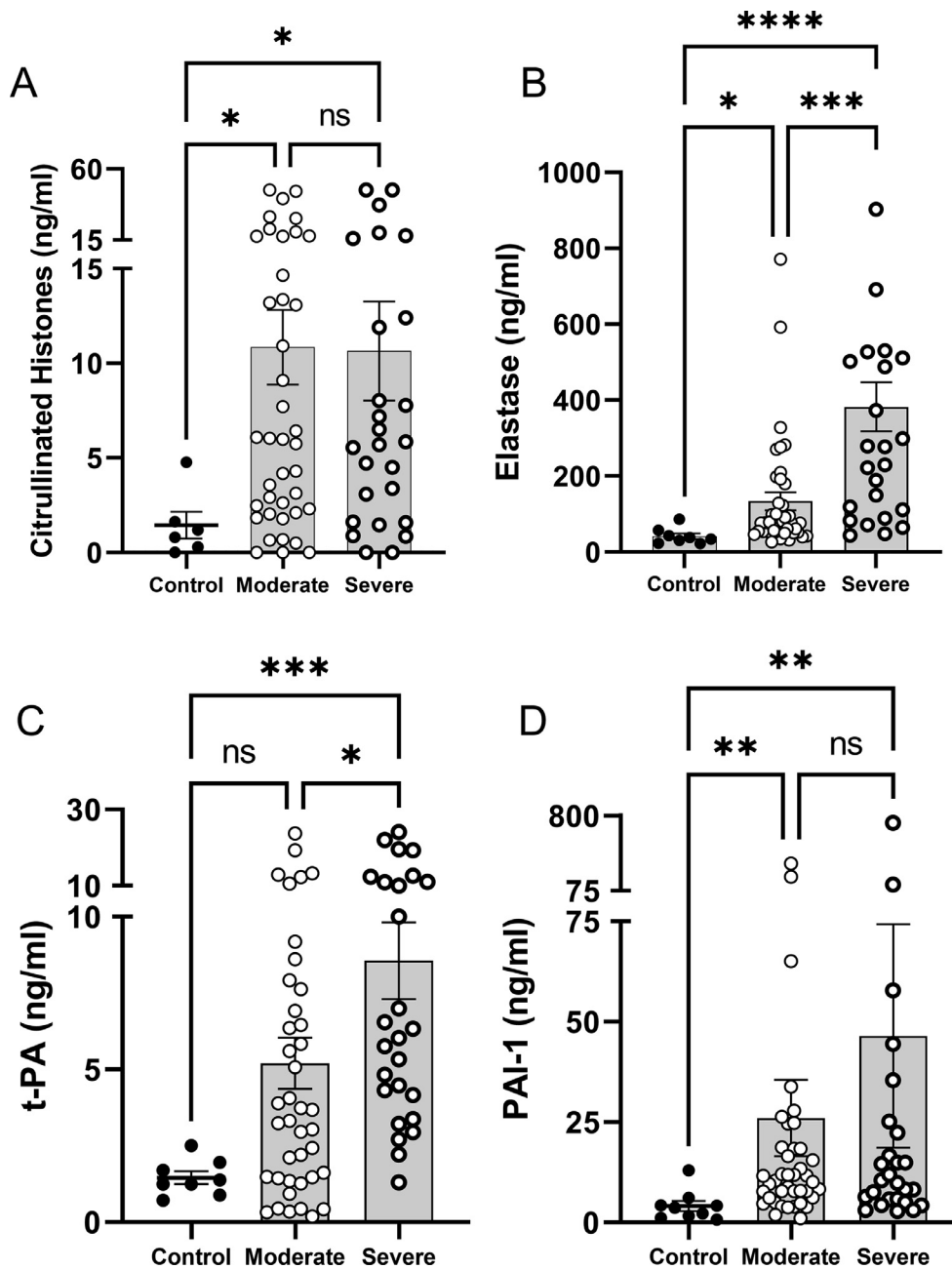


**Fig. 2.** Biomarkers of neutrophil activation and fibrinolysis in SARS-CoV-2 infection and controls. (A) Citrullinated histones, (B) Elastase, (C)  $t$ -PA, (D) PAI-1 plasma concentrations were determined by ELISA in healthy donors and COVID-19 patients. Each symbol correspond one patient. Shaded bars indicate the means, and the lines show the SEM. NS, non-significant; \* $p < 0.05$ ; \*\* $p < 0.01$ , \*\*\* $p < 0.001$ , \*\*\*\* $p < 0.0001$  (Kruskal-Wallis test, or Mann-Whitney  $U$  test).

1.2.6. Tissue factor

TF/VIIa complex initiates coagulation in normal conditions and in systemic infections [36,37]. Because FVIIa is inhibited by AT only when it is bound to TF, resulting in the accelerated dissociation of FVIIa from TF, the circulating levels of AT/FVIIa complex may reflect the degree of intravascular exposure of TF to the blood [53]. Our results show that AT/VIIa complex in plasma was higher among severe cases than normal controls ( $p = 0.03$ ) but was not significantly elevated in the moderate disease group vs controls ( $p = 0.43$ ), or moderate vs severe disease groups ( $p = 0.17$ ) (Fig. 3A).

Microparticles containing TF (MP-TF) are released from leukocytes, endothelial cells, and platelets upon cellular activation [53, 54]. We selected 8 cases from each group based on high D-dimer levels and ICU stay to determine MP-TF levels. Fig. 3B shows no difference in MP-TF in moderate vs normal controls; however, a statistically significant difference was observed between controls and severe cases ( $p = 0.025$ ). The TF-dependent activity of the assay was blocked by Ixolaris, a specific inhibitor of TF [44]. Ixolaris also prolonged the PT but not the aPTT, confirming its specificity (Fig. 3C). In addition, Ixolaris dose-dependently attenuated thrombin generation triggered by

TF in the Thrombin Generation Assay (Fig. 3D). Endogenous thrombin potential (ETP), thrombin peak (TP) and time for thrombin peak (TTP) values are respectively shown in parenthesis, with increasing concentrations of Ixolaris, as follows: 0 nM (1511 nM/min, 171 nM, 7.5 min), 2.5 nM (1182 nM/min, 102.4 nM, 9.8 min), 5 nM (912.7 nM/min, 69.67 nM, 11.3 min), 10 nM (736.8 nM/min, 51.78 nM, 13.4 min), 20 nM (496.8 nM/min, 32.44 nM, 18.6 min).

1.2.7. Association between D-dimer levels, and biomarkers of cellular activation

High D-dimers are associated with high mortality in Sars-CoV-2 infection [4]. In our cohort, heat map showed that D-dimer were significantly correlated ( $p < 0.05$ ) with angiotensin-1, angiotensin-2, AT/VIIa complex, citrullinated histones, elastase, P-selectin, thrombomodulin, t-PA, TFPI, vWF:RCo and vWF:Ag (Fig. 4A). The specific  $r$  and  $p$  values for each correlation is reported in Fig. 4B. Across all study participants, D-dimers also correlated with age ( $r = 0.46$ ,  $p < 0.001$ ), WBC ( $r = 0.38$ ,  $p = 0.001$ ), Hg ( $r = 0.49$ ,  $p < 0.001$ ), ANC ( $r = 0.45$ ,  $p < 0.001$ ), AMC ( $r = 0.32$ ,  $p = 0.01$ ) and creatinine ( $r = 0.31$ ,  $p = 0.01$ ).

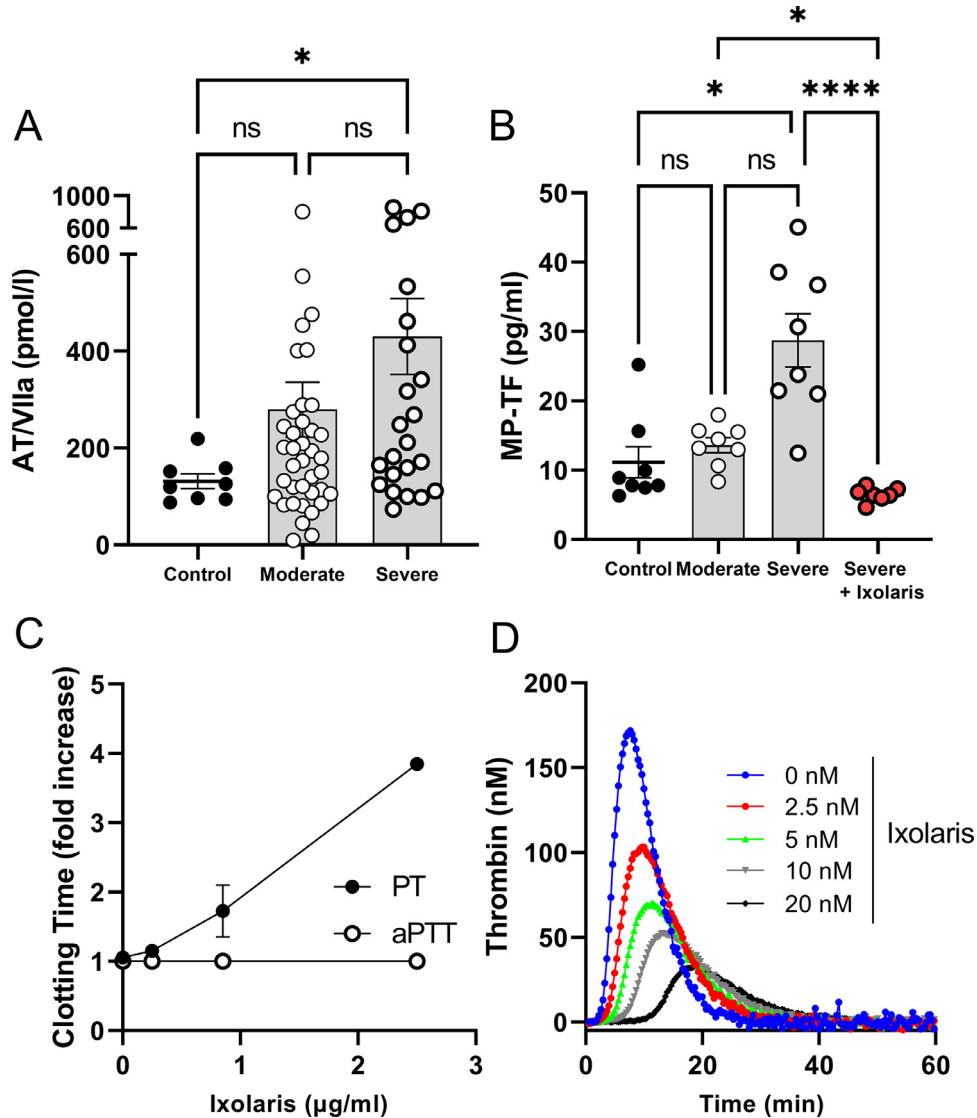
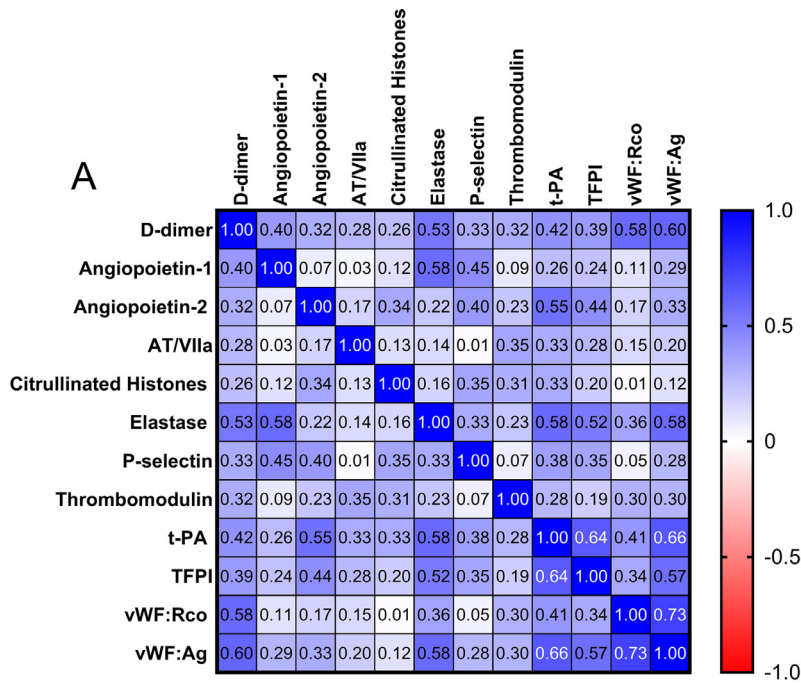


**Fig. 3.** Anti-thrombin/Factor VIIa (AT/VIIa) complex, and microparticle-TF (MP-TF) levels in SARS-CoV-2 infection and controls. (A) AT/VIIa complex and (B) MP-TF plasma levels were determined by ELISA in healthy controls and patients with COVID-19 patients. Ixolaris, a TF inhibitor, blocks MP-associated TF activity. Each symbol correspond one patient. Shaded bars indicate the means, and the lines show the SEM. (C) Ixolaris prolongs the PT, but not the aPTT. (D) Thrombin generation assay. Reactions were initiated by the addition of  $CaCl_2$ , phospholipids and TF, with and without Ixolaris, as indicated. Each curve shows the mean of triplicate reactions in pooled plasma. NS, non-significant; \*\* $p < 0.01$ , \*\*\*\* $p < 0.0001$  (Kruskall-Wallis test).



**B**

	D-dimer		Angiopoietin-1		Angiopoietin-2		AT/VIIa		Citrullinated Histones		Elastase		P-selectin		Thrombomodulin		t-PA		TFPI		vWF:Rco		vWF:Ag	
	r	p	r	p	r	p	r	p	r	p	r	p	r	p	r	p	r	p	r	p	r	p	r	p
D-dimer	1.00		0.40	<0.001	0.32	0.006	0.02	0.016	0.26	0.028	0.53	<0.001	0.33	0.004	0.32	0.005	0.42	<0.001	0.39	0.001	0.58	<0.001	0.60	<0.001
Angiopoietin-1	0.40	<0.001	1.00		0.07	0.541	0.77	0.774	0.12	0.327	0.58	<0.001	0.45	<0.001	0.09	0.453	0.26	0.026	0.24	0.041	0.11	0.347	0.29	0.011
Angiopoietin-2	0.32	0.005	0.07	0.540	1.00		0.14	0.145	0.34	0.003	0.22	0.064	0.40	<0.001	0.23	0.052	0.55	<0.001	0.44	<0.001	0.17	0.148	0.33	0.005
AT/VIIa	0.28	0.016	0.03	0.770	0.17	0.145	1.00		0.13	0.280	0.14	0.224	0.01	0.911	0.35	0.002	0.33	0.005	0.28	0.017	0.15	0.212	0.20	0.092
Citrullinated Histones	0.26	0.028	0.12	0.320	0.34	0.003	0.28	0.280	1.00		0.16	0.176	0.35	0.003	0.31	0.008	0.33	0.005	0.30	0.093	0.01	0.925	0.12	0.317
Elastase	0.53	<0.001	0.58	<0.001	0.22	0.064	0.22	0.224	0.16	0.176	1.00		0.33	0.004	0.23	0.053	0.58	<0.001	0.52	<0.001	0.36	0.002	0.58	<0.001
P-selectin	0.33	0.004	0.45	<0.001	0.40	<0.001	0.91	0.911	0.35	0.003	0.33	0.004	1.00		0.07	0.578	0.38	0.001	0.35	0.002	0.05	0.657	0.28	0.015
Thrombomodulin	0.32	0.005	0.09	0.450	0.23	0.052	0.00	0.002	0.31	0.008	0.23	0.053	0.07	0.578	1.00		0.28	0.016	0.19	0.094	0.30	0.009	0.30	0.011
t-PA	0.42	<0.001	0.26	0.020	0.55	<0.001	0.00	0.005	0.33	0.005	0.58	<0.001	0.38	0.001	0.28	0.016	1.00		0.64	<0.001	0.41	<0.001	0.66	<0.001
TFPI	0.39	0.001	0.24	0.040	0.44	<0.001	0.02	0.017	0.20	0.093	0.52	<0.001	0.35	0.002	0.19	0.094	0.64	<0.001	1.00		0.34	0.003	0.57	<0.001
vWF:Rco	0.58	<0.001	0.11	0.340	0.17	0.148	0.21	0.212	0.01	0.925	0.36	0.002	0.05	0.657	0.30	0.009	0.41	<0.001	0.34	0.003	1.00		0.73	<0.001
vWF:Ag	0.60	<0.001	0.29	0.010	0.33	0.005	0.09	0.092	0.12	0.317	0.58	<0.001	0.28	0.015	0.30	0.011	0.66	<0.001	0.57	<0.001	0.73	<0.001	1.00	

**Fig. 4.** Correlation between D-dimer and several biomarkers in SARS-CoV-2 infection. (A) Heatmap shows positive correlations indicated by the intensity in blue, as defined in the legend. (B) R value and p value for each correlation is indicated. AT/VIIa, antithrombin/Factor VIIa complex; t-PA, tissue plasminogen activator; TFPI, tissue factor pathway inhibitor; vWF:Ag, WF antigen; vWF:Rco, vWF ristocetin cofactor activity. Significance set at  $p < 0.05$  (Spearman rank coefficient correlation) (For interpretation of the references to color in this figure legend, the reader is referred to the web version of this article.)

**1.2.8. Biomarkers associated with severe disease**

A logistic regression model was generated with outcome (severe vs moderate disease) as the dependent variable, and numerous biomarkers of biochemical, hematological, inflammatory and coagulation indices as independent variables. The results of univariate analysis are shown in Table 2. D-dimers, age, platelet count, IL-6, ferritin, WBC, Hg, ANC, AMC, LDH, P-selectin, angiopoietin-1, elastase, P1 + 2, thrombomodulin, t-PA, vWF:RCo, and vWF:Ag were significantly associated with disease severity on univariate regression. When a multivariate logistic regression model was employed using only biomarkers missing fewer than 5 data points, ANC (Odds ratio, OR 2.005; 95% confidence interval, CI 1.043–3.853;  $p = 0.036$ ) and vWF:Ag (OR 1.023; 95% CI 1.000–1.047;  $p = 0.0494$ ) were independent predictors of disease severity. D-dimers were not independently predictive of severe disease when Hg, ANC, angiopoietin-1, P1 + 2, P-selectin, thrombomodulin and vWF:Ag were included in the model. Age was included as a potential variable when performing lasso regression but was not selected by the process. When setting the penalty factor for age to 0, in effect forcing age to always be included in the model, there were no significant changes in other coefficients and our interpretation of the model remained largely the same. Given the relatively small number of cases, these multivariable models should be viewed as exploratory only.

**1.2.9. Post-Mortem studies**

Nine autopsy cases were evaluated: 4 controls who died of other conditions not associated with pulmonary disease and 5 others from patients who died from COVID-19 with acute lung injury [46]. Table 3 shows the demographics, and selected clinical information, days on ventilators, presence of thrombosis, and other specifics for each case. Autopsy findings included diffuse alveolar damage, hyaline membranes, microthrombi and fibrin, neutrophilic infiltration, squamous metaplasia, multinucleated giant cells, and reactive pneumocytes as described in detail elsewhere [46]. To investigate a potential cause of an increased pro-coagulant state consistent with fibrin deposition in the lungs, we investigated the expression of procoagulant TF and anticoagulants thrombomodulin and EPCR. Fig. 5A shows the H&E of a Control case #1 with preserved lung architecture. Fig. 5B depicts COVID-19 case #1 with features associated with the infection [31–33,46]. Fig. 5C reveals that Control case#1 exhibits baseline expression of TF in the epithelial cells of the alveolar wall. In contrast, COVID-19 case#1 shows an upregulation of TF predominantly associated with the alveolar epithelium (Fig. 5D). A semi-quantitative score  $3.2 \pm 0.3$  for TF in the disease vs  $0.7 \pm 0.2$  for controls, showed a statistically significant difference with  $p = 0.015$  (Mann-Whitney U test). Fig. 5E illustrates normal expression of thrombomodulin in the alveolar capillaries of Control case #1 while Fig. 5F shows loss of

**Table 2**  
Univariate and multivariate logistic regression of association of covariates with severe disease.

Variables	Univariate analysis			Multivariate analysis		
	OR	95% CI	p value	OR	95% CI	p value
ADAMTS13 (%)	0.984	0.961–1.008	0.1819			
Age (yo)	1.056	1.021–1.093	0.0016 *			
ALC (K/ $\mu$ l)	0.613	0.284–1.322	0.2123			
AMC (K/ $\mu$ l)	16.056	1.215–212.156	0.0350 *			
ANC (K/ $\mu$ l)	1.842	1.361–2.493	0.0001 *	2.005	1.043–3.853	0.0369 *
Angiopoietin-1 (ng/ml)	1.375	1.118–1.689	0.0025 *	1.147	0.776–1.694	0.4926
Angiopoietin-2 (ng/ml)	1.004	0.952–1.059	0.8815			
aPTT (s)	0.964	0.848–1.097	0.5794			
AT/VII (pm/L)	1.001	1.000–1.003	0.1330			
BMI	1.018	0.969–1.070	0.4798			
Citrullinated Histones (ng/ml)	0.999	0.960–1.039	0.9517			
Creatinine (mg/dl)	1.196	0.781–1.832	0.4099			
CRP (mg/dl)	1.042	0.995–1.091	0.0801			
D-dimer (mg/ml)	3.135	1.512–6.501	0.0021 *	1.149	0.582–2.270	0.6891
Elastase (ng/ml)	1.005	1.002–1.008	0.0022 *			
Ferritin (ng/ml)	1.001	1.000–1.001	0.0257 *			
Fibrinogen (mg/dl)	1.002	0.999–1.006	0.1839			
Hemoglobin (g/dl)	0.679	0.510–0.906	0.0085 *	0.637	0.356–1.142	0.1303
Interleukin-6 (pg/ml)	1.016	1.002–1.029	0.0225 *			
LDH (U/L)	1.004	1.001–1.006	0.0037 *			
P1+2 (pmol/L)	0.999	0.999–1.000	0.0070 *	0.999	0.997–1.000	0.0820
PAI-1 (ng/ml)	1.002	0.997–1.007	0.4435			
Platelet (K/ $\mu$ l)	1.006	1.000–1.012	0.0332 *			
P-selectin (pg/ml)	1.013	1.001–1.025	0.0287 *	1.009	0.988–1.031	0.4018
PT (sec)	0.957	0.828–1.106	0.5544			
sEPCR (ng/ml)	1.000	1.000–1.001	0.5674			
TFPI (ng/ml)	1.049	0.999–1.103	0.0569			
Thrombomodulin (pg/ml)	1.269	1.028–1.568	0.0269 *	1.051	0.717–1.541	0.7977
tPA (ng/ml)	1.105	1.008–1.211	0.0326 *			
vWF:Ag (%)	1.022	1.010–1.034	0.0003 *	1.023	1.000–1.047	0.0494 *
vWF:RCo (%)	1.024	1.006–1.041	0.0071 *			
WBC (K/ $\mu$ l)	1.613	1.258–2.069	0.0002 *			

CI, confidence interval; OR, odds ratio. The OR indicates the estimated increase in the log odds of disease severity per unit increase for each continuous variable.

thrombomodulin in COVID-19 case #1. A score of  $1.6 \pm 0.2$  for thrombomodulin in the disease vs  $3.5 \pm 0.2$  for controls was also significant, with  $p = 0.008$ . Fig. 5G highlights normal expression of EPCR in the endothelium of medium-to-large size vessels, but not in capillaries in Control case#1. EPCR expression seems variable in COVID-19 case#1 (Fig. 5H). An overall score of  $3.8 \pm 0.2$  for EPCR in the disease vs  $3.7 \pm 0.5$  for controls was statistically non-significant ( $p = NS$ ).

#### 1.2.10. Cellular sources of tissue factor

In order to determine the cell origin of TF expression, SARS-CoV-2 cases #1 and #2 were stained with AE1/AE3 to mark epithelial cells and CD68 to highlight macrophages. Platelet thrombi was detected with CD61. Fig. 6A shows H&E for case#1 where reactive pneumocytes are noted. Fig. 6B reveals H&E for case #2 with abundant intra-alveolar macrophages, and multinucleated giant cells (*inset*). Fig. 6C and D illustrate, respectively, marked membrane staining of TF in cells morphologically consistent with epithelial cells in both COVID-19 cases #1 and #2. In contrast, endothelial cells staining was equivocal for TF. Fig. 6E and F confirm, respectively, that TF-positive cells are positive for AE1/AE3 confirming their epithelial cell derivation (e.g. pneumocytes). Fig. 6G depicts staining of few intra-alveolar macrophages with CD68 for COVID-19 case #1, which were very abundant in COVID-19 case #2 (Fig. 6H). Although macrophages (Fig. 6D) and endothelial cells (not shown) seem negative for TF staining, a low level of expression in these cells cannot be excluded. Figs. 6I and 6J highlight, respectively numerous platelet thrombi stained with CD61 in both COVID-19 cases #1 and #2 [55]. Platelet thrombi were also found in COVID-19 cases #3, #4 and #5, but not in controls (not shown).

Fig. 7 illustrates the role of immunothrombosis and Virchow's triad in the coagulopathy of SARS-CoV-2 infection.

## 2. Discussion

Our results show that the coagulation disorder in SARS-CoV-2 infection is multifactorial and accompanied by endothelial cells, neutrophil and platelet activation, in addition to compensatory fibrinolysis [4–9]. In most patients, abnormalities in the coagulogram are mild with PT, fibrinogen and platelet counts within the normal range or borderline normal, with a DIC score of  $\leq 3$ . This picture is in keeping with a compensated state [51,56]. In these cases, a continuous or intermittent slow rate of initiation of intravascular coagulation occurs and may or may never undergo decompensation to acute DIC. Under these conditions, control mechanisms (e.g. anticoagulants) may effectively prevent severe clinical manifestations, such as bleeding and hemorrhage. This picture is typically seen in our patients, and is very much in contrast with acute (overt) DIC where a trigger for coagulation activation persists, inhibitors are gradually exhausted, resulting in a “consumptive coagulopathy” usually present in sepsis, thus differentiating both conditions [51,56,57]. However, the degree to which anticoagulation therapy (received by all COVID-19 patients in our cohort) may have prevented decompensation to acute DIC is unknown. Also, absence of statistically significant difference in thrombosis in moderate vs severe disease group may be due to a small size of our cohort.

Several studies have shown that endothelial cell activation is a hallmark of COVID-19 infection, as a result of multiple mechanisms [10–15]. Upon cellular activation, high molecular weight vWF multimers are released by endothelium, processed by ADAMTS13, and necessary for normal hemostasis [50]. Our cohort shows elevated vWF:RCo and vWF:Ag and a trend towards lower-ADAMTS13 activity in severe disease. Furthermore, a positive correlation of high D-dimers with vWF:Ag and vWF:RCo was found here, and we identified

**Table 3**  
Demographic and clinical information for autopsy cases.

Control	Age (yo)	Sex (M/F)	PMI (hrs)	CV+To death (days)	Ventilator(days)	Comorbidities	Acute Lung Injury	Thrombosis	Other major findings	Cause of death
Control-1	79	M	15	None	8	Aortic aneurysm, hypertension, AF	No	No	CAD, focal acute pneumonia, kidney infarct, strokes	Anoxic brain injury, PEA, CAD
Control-2	85	F	12	None	n/a	Metastatic prostate cancer	No	No	Cystitis, pyelonephritis	Sepsis due to UTI due to obstruction
Control-3	48	M	39	None	< 1	18 cm retroperitoneal mass	No	No	Focal acute pneumonia, abdominal hemorrhage, ischemic bowel	Intraabdominal hemorrhage post abdominal resection
Control-4	81	F	30	None	n/a	Dementia, heart failure, CAD, CKD	Yes, also organizing	Yes, cardiac only with ischemia	Ischemic cardiomyopathy and amyloidosis, Alzheimer	Sepsis due to UTI
COVID-19	Age (yo)	Sex (M/F)	PMI (hrs)	CV + To death (days)	Ventilator (days)	Comorbidities	Acute Lung Injury	Thrombosis	Other major findings	Cause of death
Covid-1	64	F	23	7	1	Hypertension, diabetes	Yes	Yes	None	COVID-ALI
Covid-2	67	M	18	15	11	Asthma	Yes	Yes	None	COVID-ALI
Covid-3	62	F	19	19	7	Diabetes, Stroke	Yes	Yes	Steatosis	COVID-ALI
Covid-4	84	M	17	21	15	Myocardium infection, Alzheimer's Disease, Parkinson Disease	Yes	Yes	Shock kidney	COVID-ALI
COVID-5	82	F	50	6	n/a	End-stage renal disease	Yes	Yes	Obesity, ESRD, CAD, sub-acute-to-old MI with adjacent thrombi	COVID-ALI

ALI, acute lung injury; AF, atrial fibrillation; CAD, coronary artery disease; CV + To death, time from positivity for COVID-19 to death. ESRD, end-stage renal disease; PEA, pulseless electric activity; PMI, postmortem interval (time from death to autopsy). UTI, urinary tract infection; CKD, chronic kidney disease; n/a, not available.

vWF:Ag as an independent marker associated with disease severity, also reported by others [10,15,58,59]. It has been suggested that an imbalance between high molecular weight vWF multimers and ADAMTS13 may facilitate vWF interaction with circulating platelets and increase the risk of microthrombosis in SARS-CoV-2 patients, among other mechanisms [10,15,58,59].

Thrombomodulin forms a complex with thrombin, and in the presence of EPCR it activates protein C into activated protein C (APC) [41]. Our findings reveal an increase in plasma thrombomodulin, indicating loss of this anticoagulant from the endothelial cell surface. In this respect, high thrombomodulin is associated with severe disease here and has predictive value for mortality in COVID-19 infection elsewhere [15,57]. Our results also demonstrated a concomitant increase in plasma sEPCR and thus suggest that endothelial expression of both receptors of the protein C pathway were affected, pointing towards a potentially impaired ability of the endothelium to generate and mediate APC cellular functions which reportedly reduce inflammation, apoptosis, and stabilize endothelial and epithelial barriers [40,41]. While most studies show mild changes in PC levels [4–8], a recent paper reported lower protein C in COVID-19 patients, resulting in an acquired protein C deficiency-like picture that may contribute to development of a thrombogenic state and worsening of patient's clinical condition [60]. We also found that TFPI, the main inhibitor of the extrinsic pathway [36,37] was markedly elevated in moderate and severe disease, indicating loss from the endothelium. This is in keeping with an unchecked TF pathway; of note, impaired TFPI activity may facilitate the kinetics of FVIIa/TF/FXa complex formation and protease activated receptor (PAR) activation leading to an inflammatory phenotype [51,54]. As TFPI is mainly associated with endothelial cells through binding to heparan sulfate proteoglycans [36,37], a main component of the glycocalyx at the surface of endothelial cells, these results also support the notion that glycocalyx disruption is an important feature of severely ill patients [61].

Angiotensins are released by and modulate endothelial cells functions [52]. Our results show a marked elevation of angiotensin-2 in both moderate and severe disease, in contrast to angiotensin-1. These results have several implications since the angiotensin-2 receptor, Tie-2 is expressed in epithelial cells, macrophages and in vessels of the lung from COVID-19 patients [62]. It has been suggested that the combination of abnormal expression of Tie-2 and angiotensin-2 is associated with extensive airway remodeling and form the basis for acutely progressive respiratory distress in SARS-CoV-2 patients [62]. This assertion is corroborated by an association of angiotensin-2 with in-hospital mortality and non-resolving pulmonary disease [58,62]. Our results also underscore the potential role of endothelial cells in coagulation activation based on a positive correlation of D-dimer with angiotensin-2 and multiple others endothelial cell markers (angiotensin-1, P-selectin, thrombomodulin, TFPI, vWF:Ag, vWF:RCo, t-PA, P-selectin). In addition, the significance of microvascular damage is highlighted by other markers of endothelial cell activation and angiogenesis, the presence of circulating endothelial cells, and an association of endothelium activation with disease severity including respiratory and multiorgan failure [10–15,11–13,61,63]. Moreover, it is congruent with a pathologic process affecting endothelial cells given the vast surface it occupies estimated in more than 1000 m<sup>2</sup>, or 10<sup>12</sup> endothelial cells (there are ~ 10<sup>10</sup> blood monocytes) weighting in excess of 100 gs in the adult human [64].

Neutrophils have a critical role in immunothrombosis through interaction with activated endothelial cells, and release of NETs [21–27]. We observed an increase of citrullinated histones H3 (a marker for NETs) and elastase in both moderate and severe cases. Both biomarkers positively correlate with D-dimer in our cohort, with high ANC showing an independent association with severity. Other studies have demonstrated that the lungs have numerous micro-vessels containing NETs associated with endothelial damage

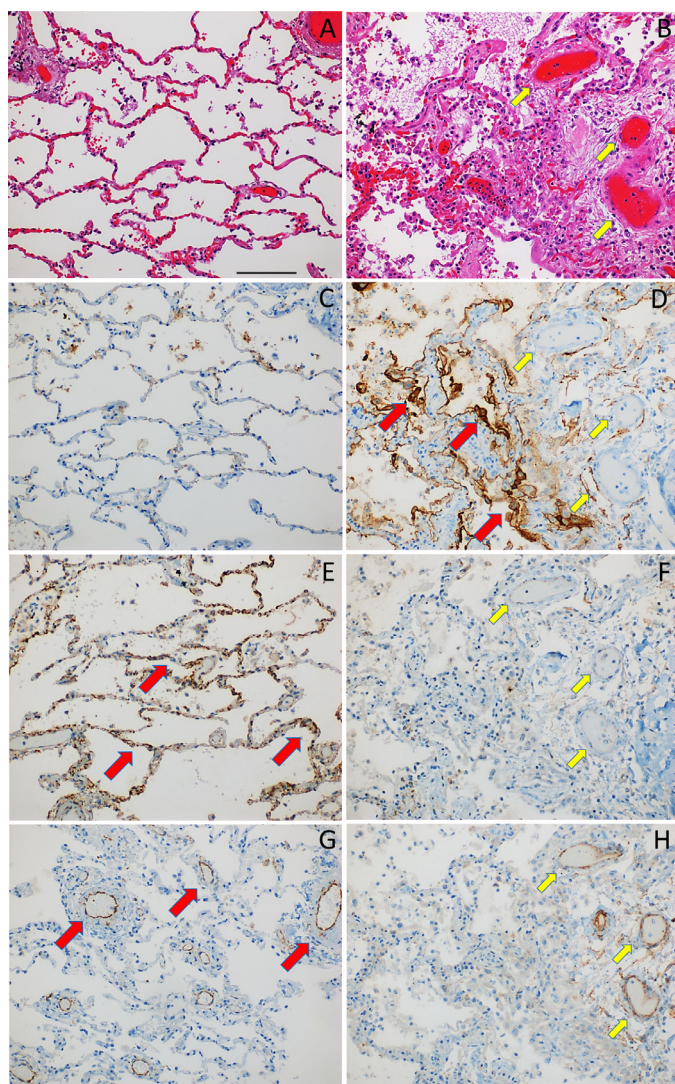


**Fig. 5.** Tissue Factor (TF), thrombomodulin and EPCR in the lung of SARS-CoV-2 infection and controls. (A) Control case #1. H&E shows preserved alveolar structures. (B) COVID-19 case #1. H&E shows loss of normal lung architecture and changes associated with the disease. (C) Control case #1. TF expression is minimally detected in the alveolar epithelium. (D) COVID-19 case #1. Marked upregulation of TF in epithelial cells. (E) Control case #1. Preserved thrombomodulin expression in the endothelial cells of alveolar capillaries. (F) COVID-19 case #1. Markedly attenuated staining of thrombomodulin. (G) Control case#1. Preserved EPCR expression in the endothelial cells of larger vessels. (H) COVID-19 case #1. Variable/preserved staining of EPCR in large vessels. The yellow arrows show 3 vessels in consecutive sections of COVID-19 case #1, allowing comparison of similar areas for all immunostains. The red arrows indicate expression of the proteins of interest. All images ( $\times 200$ ). Bar represents  $100 \mu\text{m}$  (For interpretation of the references to color in this figure legend, the reader is referred to the web version of this article).

which may promote activation of the intrinsic pathway [24,26,27]. This response may be amplified by activation of the extrinsic pathway by TF associated with platelet-monocyte aggregates, neutrophils, or induced by complement activation, among other mechanisms [4–7,21,28,65]. In this respect, the relative contribution of TF pathway in coagulation dysregulation was determined by AT/FVIIa since this biomarker may reflect the degree of intravascular exposure of TF to the blood [53]. Our results show that AT/FVIIa is elevated in severe cases, corroborating the view that TF expression plays a relatively major role in advanced disease. Likewise, MP-TF, a marker of cellular activation in inflammatory states [66], is increased in patients with severe COVID-19 infection. MP-TF was functionally active as FXa generation was blocked by Ixolaris, a specific TF inhibitor [44]. These

findings are relevant as MP-TF positively correlates with leukocytes, D-dimer, inflammatory parameters, and is associated with an increased thrombotic risk, disease severity and mortality in SARS-CoV-2 [67,68]. With respect to cellular sources for TF, there is evidence for participation of neutrophils [21], platelet-monocyte aggregates and [28] macrophages [69] although transcripts for TF were not upregulated in monocytes in SARS-CoV-2 [38], in contrast with sepsis [17,51,70]. At last, our univariate analysis supports the view that coagulation dysregulation in COVID-19 infection has a multifactorial etiology.

Activation of the coagulation cascade in the disease, confirmed here by elevated P1 + 2, is accompanied by compensatory fibrinolysis, secondary to t-PA-dependent plasmin generation and fibrin degradation resulting in D-dimers. Our studies demonstrated elevated t-PA mainly in the severe disease group. Therefore, it is unlikely that a systemic or complete fibrinolytic shutdown takes place in the disease, as elevated D-dimers—a typical feature of the disease [4–9] requires biologically active/uninhibited t-PA. With respect to regulation of fibrinolysis, PAI-1 the main inhibitor of t-PA is elevated in moderate and in severe disease consistent with an endotheliopathy, as the endothelium is a primary source of PAI-1. It may also explain the moderate augmentation of D-dimers [4–9], compared to sepsis [57].

Notably, postmortem studies in our cohort showed upregulation of TF expression in SARS-CoV-2 patients who developed ALI. On the other hand, TF staining was marginally detected in our controls. TF expression was present in epithelial cells but not in macrophages, multinucleated giant cells or endothelial cells. A low level of expression in these cells, however, cannot be excluded. Remarkably, a recent study reported that lung epithelial cells derived from BAL of COVID-19 patients, as opposed to other cell types [38], significantly upregulate TF gene based on single cell RNA sequencing and uniform manifold approximation and projection (UMAP) representation [71]. Furthermore, *in vitro* SARS-CoV-2 infection of primary human lung epithelial cells confirms transcriptional upregulation of TF [38]. Therefore, the pulmonary epithelium, known as a primary source of procoagulant stimulus [72–76]. Conceivably, dysregulated TF expression in epithelial cells, and possibly other cell types, promote local coagulation and inflammatory responses through PARs at sites of alveolar epithelial cell and capillary/endothelium damage leading to sustained coagulation-inflammation cycle [4–7,9,54,73,77]. These responses are potentially amplified by loss of thrombomodulin demonstrated here by immunostains. Of note, transcriptional analysis of the BAL from COVID-19 patients showed downregulated mRNA levels for thrombomodulin and EPCR [39]. It is plausible that impaired protein C activation, together with upregulation of TF, shifts local hemostasis towards a procoagulant state. This interpretation is supported by detection of markers of coagulation and complement cascade activation, cytokines, chemokines and growth factors in the BAL of severe COVID-19 patients [77]. It is also supported by fibrin deposition and platelet thrombi particularly in the vascular beds of the lung, although other organs are also involved based on postmortem studies (e.g. liver, kidney, heart) [31–35].

It is important to recognize that the lung is highly vascularized and changes in pulmonary vascular endothelium may promote continuous and/or intermittent thrombin generation that may reach the systemic circulation but neutralized by plasma anticoagulants. This explains why a consumption coagulopathy does not occur in most cases, unless a secondary infection and/or associated liver failure are present. Altogether, it is evident that endothelial cell injury, hypercoagulability and venous stasis are readily identified in COVID-19 patients. These 3 components define the Virchow's triad [78], and when combined with heightened immunothrombosis seem to distinguish severe COVID-19 from H1N1 influenza pneumonia [27,79]. It

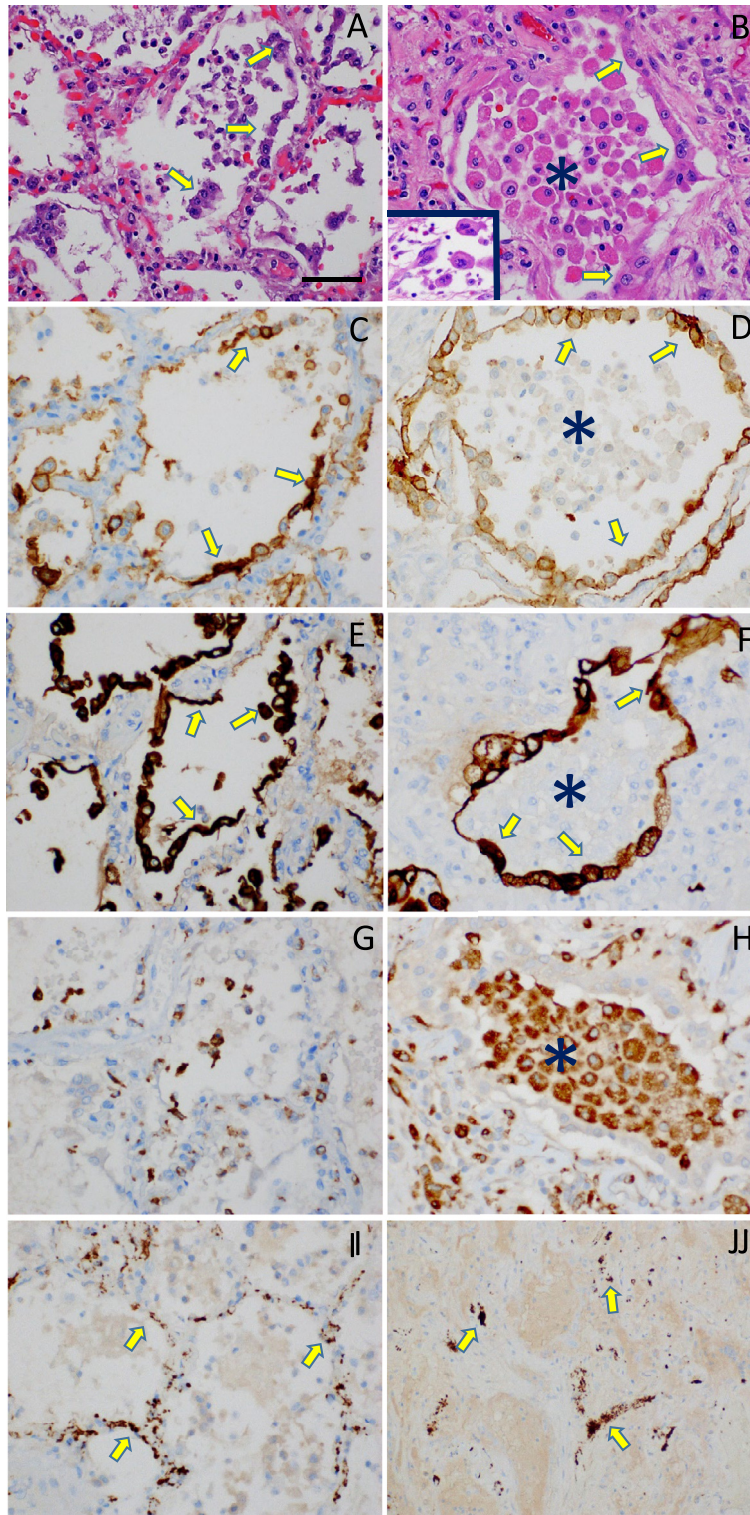


**Fig. 6.** Cellular sources of Tissue Factor (TF) in the lung of 2 cases of SARS-CoV-2 infection. (A) COVID-19 case #1. H&E shows reactive pneumocytes (arrows). (B) COVID-19 case #2. Accumulation of intraalveolar macrophages, reactive pneumocytes (arrow), and multinucleated giant cells (inset). (C) and (D) COVID-19 case #1 and case #2, respectively. Marked upregulation of TF (arrows) shown as membrane staining in epithelial cells from both cases. (E) and (F) COVID-19 case #1 and case #2, respectively. Cyokeratin staining (arrows) of epithelial cells with AE1/AE3 in both cases. (G) COVID-19 case #1. CD68 shows few intra-alveolar macrophages. (H) COVID-19 case #2. CD68 confirms abundant intra-alveolar macrophages. For B, D, F and H, asterisks show intra-alveolar macrophages. (I) and (J) COVID-19 case #1 and case #2, respectively. CD61 staining shows intravascular platelet thrombi (arrows) in both cases. All images (x400). Bar represents 50  $\mu$ m.

may also explain the high incidence of thrombosis in SARS-CoV2 infection compared to other viral pulmonary infections.

There are a few important limitations of this work. First, this was a small, single-center study, which potentially limits both our ability to define multivariable associations as well as potential generalizability.

Second, the universal use of anticoagulation in our COVID-19 patients may have altered our findings. However, the impact of anticoagulation would likely have attenuated the hemostatic activation we observed, biasing toward the null. Third, we have not studied patients with severe lung disease due to conditions other than

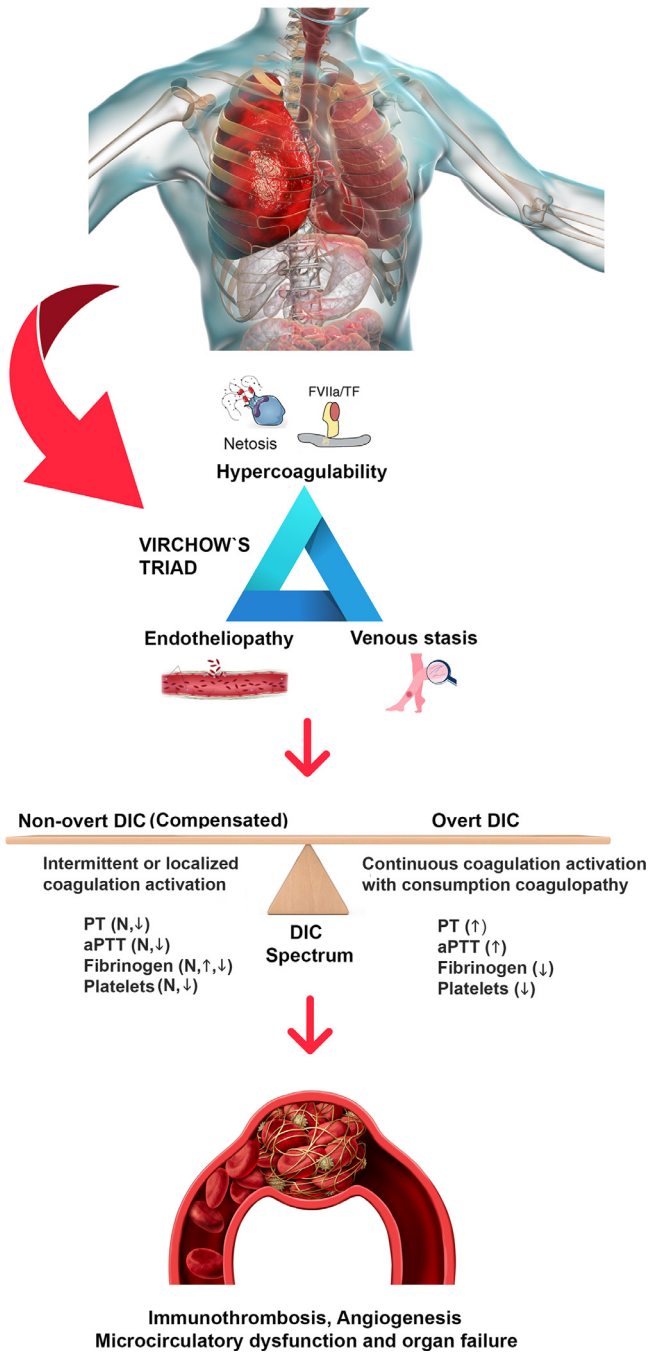


**Fig. 7.** Immunothrombosis and Virchow's triad in SARS-CoV-2 infection. Multiple mechanisms (e.g. viral cytopathic, complement activation, NETs, hypoxia, pyroptosis, "cytokine storm") lead to TF expression in the epithelial cells and possibly other cell types. It also promotes activation of endothelial cells resulting in immunothrombosis with release of NETs (Netosis). Given the tropism of SARS-CoV-2, these events are particularly intense in (but not restricted to) the lungs and creates a marked inflammatory response. This process is dysregulated resulting in an exacerbated coagulation-inflammation-angiogenesis cycle. Excessive thrombin generation overcomes inhibition by local anticoagulants whose functions are impaired due to endothelial cell damage with loss of thrombomodulin and TFPI. As a result fibrin deposition and platelet thrombi occur. Accordingly, 3 component of the Virchow's triad, namely hypercoagulability, endothelium activation, and blood stasis are present in most patients and may predispose to thrombosis. Excess thrombin in the lung may also reach the systemic circulation and is likely neutralized by natural anticoagulants, preventing a consumption coagulopathy, unless superimposed with bacterial sepsis and/or liver dysfunction. This process is typical of a compensated coagulopathy (non-overt DIC) [51,56], with compensatory fibrinolysis explaining elevated D-dimers secondary to plasmin degradation of fibrin. In extreme conditions, impaired microcirculation results in organ failure, high morbidity and mortality.

COVID-19, such as those with ALI due to other etiologies. In this respect, ALI has been associated with coagulation activation before in several other studies in humans and mice, indicating that abnormal TF expression is not specific for COVID-19 infection [27,72–76,79]. In conclusion, this study helps to clarify the potential role of immunothrombosis combined with the Virchow's triad in the pathogenesis of COVID-19 associated ALI. Whether these findings may help to tailor therapeutic strategies for COVID-19 [80] or other similar pandemic viruses deserves further study.

**Declaration of Competing Interest**

None of the authors have competing interest.

**Funding**

This study was supported by the John Hopkins University School of Medicine Grant 80053630 (I.F.).

**Data sharing statement**

All data used and obtained in this study are available in the manuscript and supporting information.

**Acknowledgment**

We thank all physicians and medical staff involved in patient care, and all the technicians of the Core Lab and Department of Pathology for their support during the coronavirus disease 2019 (COVID-19) pandemic.

**Supplementary materials**

Supplementary material associated with this article can be found in the online version at doi:10.1016/j.eclinm.2021.101069.

**References**

- [1] Dong E, Du H, Gardner L. An interactive web-based dashboard to track COVID-19 in real time. *Lancet Infect Dis* 2020;20(5):533–4.
- [2] Guan WJ, Ni ZY, Hu Y, et al. Clinical characteristics of coronavirus disease 2019 in China. *N Engl J Med* 2020;382(18):1708–20.
- [3] Zhou F, Yu T, Du R, et al. Clinical course and risk factors for mortality of adult inpatients with COVID-19 in Wuhan, China: a retrospective cohort study. *Lancet* 2020;395(10229):1054–62.
- [4] McFadyen JD, Stevens H, Peter K. The emerging threat of (Micro)thrombosis in COVID-19 and its therapeutic implications. *Circ Res* 2020;127(4):571–87.
- [5] Wiersinga WJ, Rhodes A, Cheng AC, Peacock SJ. Pathophysiology PHC. Transmission, diagnosis, and treatment of coronavirus disease 2019 (COVID-19): a review. *JAMA* 2020;324(8):782–93.
- [6] Lax SF, Skok K, Zechner P, et al. Pulmonary arterial thrombosis in COVID-19 with fatal outcome: results from a prospective, single-center. *Clinicopathol Case Ser Ann Intern Med* 2020;173(5):350–61.
- [7] Bonaventura A, Vecchie A, Dagna L, et al. Endothelial dysfunction and immunothrombosis as key pathogenic mechanisms in COVID-19. *Nat Rev Immunol* 2021;21(5):319–29.
- [8] Iba T, Levy JH, Levi M, Thachil J. Coagulopathy in COVID-19. *J Thromb Haemost* 2020;18(9):2103–9.
- [9] Boonyasai RT, Murthy VK, Yuen-Gee Liu G, et al. Venous thromboembolism in hospitalized patients with COVID-19 receiving prophylactic anticoagulation. *Mayo Clin Proc* 2020;95(10):2291–3.
- [10] Philippe A, Chocron R, Gendron N, et al. Circulating von willebrand factor and high molecular weight multimers as markers of endothelial injury predict COVID-19 in-hospital mortality. *Angiogenesis* 2021;24(3):505–17.
- [11] Pine AB, Meizlish ML, Goshua G, et al. Circulating markers of angiogenesis and endotheliopathy in COVID-19. *Pulm Circ* 2020;10(4):2045894020966547.
- [12] Guervilly C, Burtsey S, Sabatier F, et al. Circulating endothelial cells as a marker of endothelial injury in severe COVID-19. *J Infect Dis* 2020;222(11):1789–93.
- [13] Ackermann M, Verleden SE, Kuehnel M, et al. Pulmonary vascular endothelialitis, thrombosis, and angiogenesis in COVID-19. *N Engl J Med* 2020;383(2):120–8.
- [14] Varga Z, Flammer AJ, Steiger P, et al. Endothelial cell infection and endotheliitis in COVID-19. *Lancet* 2020;395(10234):1417–8.

- [15] Goshua G, Pine AB, Meizlish ML, et al. Endotheliopathy in COVID-19-associated coagulopathy: evidence from a single-centre, cross-sectional study. *Lancet Haematol* 2020;7(8):e575–e82.
- [16] Engelmann B, Massberg S. Thrombosis as an intravascular effector of innate immunity. *Nat Rev Immunol* 2013;13(1):34–45.
- [17] Opal SM, Esmon CT. Bench-to-bedside review: functional relationships between coagulation and the innate immune response and their respective roles in the pathogenesis of sepsis. *Crit Care* 2003;7(1):23–38.
- [18] Castanheira FVS, Kubes P. Neutrophils and NETs in modulating acute and chronic inflammation. *Blood* 2019;133(20):2178–85.
- [19] Thiam HR, Wong SL, Wagner DD, Waterman CM. Cellular mechanisms of NETosis. *Annu Rev Cell Dev Biol* 2020;36:191–218.
- [20] Sivanandham R, Brocca-Cofano E, Krampe N, et al. Neutrophil extracellular trap production contributes to pathogenesis in SIV-infected nonhuman primates. *J Clin Invest* 2018;128(11):5178–83.
- [21] Skendros P, Mitsios A, Chrysanthopoulou A, et al. Complement and tissue factor-enriched neutrophil extracellular traps are key drivers in COVID-19 immunothrombosis. *J Clin Invest* 2020;130(11):6151–7.
- [22] Nicolai L, Leunig A, Brambs S, et al. Immunothrombotic dysregulation in COVID-19 pneumonia is associated with respiratory failure and coagulopathy. *Circulation* 2020;142(12):1176–89.
- [23] Meizlish ML, Pine AB, Bishai JD, et al. A neutrophil activation signature predicts critical illness and mortality in COVID-19. *Blood Adv* 2021;5(5):1164–77.
- [24] Middleton EA, He XY, Denorme F, et al. Neutrophil extracellular traps contribute to immunothrombosis in COVID-19 acute respiratory distress syndrome. *Blood* 2020;136(10):1169–79.
- [25] Leppkes M, Knopf J, Naschberger E, et al. Vascular occlusion by neutrophil extracellular traps in COVID-19. *EBioMed* 2020;58:102925.
- [26] Veras FP, Pontelli MC, Silva CM, et al. SARS-CoV-2-triggered neutrophil extracellular traps mediate COVID-19 pathology. *J Exp Med* 2020;217(12):e20201129.
- [27] Nicolai L, Leunig A, Brambs S, et al. Vascular neutrophilic inflammation and immunothrombosis distinguish severe COVID-19 from influenza pneumonia. *J Thromb Haemost* 2021;19(2):574–81.
- [28] Hottz ED, Azevedo-Quintanilha IG, Palhinha L, et al. Platelet activation and platelet-monocyte aggregate formation trigger tissue factor expression in patients with severe COVID-19. *Blood* 2020;136(11):1330–41.
- [29] Gavrilaki E, Brodsky RA. Severe COVID-19 infection and thrombotic microangiopathy: success does not come easily. *Br J Haematol* 2020;189(6):e227–e30.
- [30] Merrill JT, Erkan D, Winakur J, James JA. Emerging evidence of a COVID-19 thrombotic syndrome has treatment implications. *Nat Rev Rheumatol* 2020;16(10):581–9.
- [31] Carsana L, Sonzogni A, Nasr A, et al. Pulmonary post-mortem findings in a series of COVID-19 cases from Northern Italy: a two-centre descriptive study. *Lancet Infect Dis* 2020;20(10):1135–40.
- [32] Hanley B, Naresh KN, Roufosse C, et al. Histopathological findings and viral tropism in UK patients with severe fatal COVID-19: a post-mortem study. *Lancet Microbe* 2020;1(6):e245–e53.
- [33] Schaefer IM, Padera RF, Solomon IH, et al. *In situ* detection of SARS-CoV-2 in lungs and airways of patients with COVID-19. *Mod Pathol* 2020;33(11):2104–14.
- [34] Tian S, Xiong Y, Liu H, et al. Pathological study of the 2019 novel coronavirus disease (COVID-19) through postmortem core biopsies. *Mod Pathol* 2020;33(6):1007–14.
- [35] Bradley BT, Maioli H, Johnston R, et al. Histopathology and ultrastructural findings of fatal COVID-19 infections in Washington State: a case series. *Lancet* 2020;396(10247):320–32.
- [36] Broze GJ, Girard TJ. Tissue factor pathway inhibitor: structure-function. *Front Biosci (Landmark Ed)* 2012;17:262–80.
- [37] Wood JP, Ellery PE, Maroney SA, Mast AE. Biology of tissue factor pathway inhibitor. *Blood* 2014;123(19):2934–43.
- [38] FitzGerald ES, Chen Y, Fitzgerald KA, Jamieson AM. Lung epithelial cell transcriptional regulation as a factor in COVID-19 associated coagulopathies. *Am J Respir Cell Mol Biol* 2021;64(6):687–97.
- [39] Mast AE, Wolberg AS, Gailani D, et al. SARS-CoV-2 suppresses anticoagulant and fibrinolytic gene expression in the lung. *Elife* 2021;10:e64330.
- [40] Giri H, Panicker SR, Cai X, Biswas I, Weiler H, Rezaie AR. Thrombomodulin is essential for maintaining quiescence in vascular endothelial cells. *Proc Natl Acad Sci U S A* 2021;118(11):e2022248118.
- [41] Esmon CT. Protein C anticoagulant system-anti-inflammatory effects. *Semin Immunopathol* 2012;34(1):127–32.
- [42] WHO. Clinical management of COVID-19: living guidance. Geneva: World Health Organization; 2021. p. 2021.
- [43] Chen P, Jani J, Streiff MB, Zheng G, Kickler TS. Evaluation of global hemostatic assays in response to factor VIII Inhibitors. *Clin Appl Thromb Hemost* 2019;25:1076029619836171.
- [44] Francischetti IM, Valenzuela JG, Andersen JF, Mather TN, Ribeiro JM. Ixolaris, a novel recombinant tissue factor pathway inhibitor (TFPI) from the salivary gland of the tick, *Ixodes scapularis*: identification of factor X and factor Xa as scaffolds for the inhibition of factor VIIa/tissue factor complex. *Blood* 2002;99(10):3602–12.
- [45] Gando S, Levi M, Toh CH. Disseminated intravascular coagulation. *Nat Rev Dis Primers* 2016;2:16037.
- [46] Hooper JE. Rapid autopsy programs and research support: the Pre- and Post-COVID-19 environments. *AJSP Rev Rep* 2021;26(2):100–7.
- [47] Spyropoulos AC, Levy JH, Ageno W, et al. Scientific and standardization committee communication: clinical guidance on the diagnosis, prevention, and treatment of venous thromboembolism in hospitalized patients with COVID-19. *J Thromb Haemost* 2020;18(8):1859–65.
- [48] Jones AE, Trzeciak S, Kline JA. The sequential organ failure assessment score for predicting outcome in patients with severe sepsis and evidence of hypoperfusion at the time of emergency department presentation. *Crit Care Med* 2009;37(5):1649–54.
- [49] Masias C, Cataland SR. The role of ADAMTS13 testing in the diagnosis and management of thrombotic microangiopathies and thrombosis. *Blood* 2018;132(9):903–10.
- [50] Monroe DM, Hoffman M. What does it take to make the perfect clot? *Arterioscler Thromb Vasc Biol* 2006;26(1):41–8.
- [51] Ruf W. Protease-activated receptor signaling in the regulation of inflammation. *Crit Care Med* 2004;32(5):S287–92 Suppl.
- [52] Parikh SM. Angiopoietins and Tie2 in vascular inflammation. *Curr Opin Hematol* 2017;24(5):432–8.
- [53] Spiezia L, Rossetto V, Campello E, et al. Factor VIIa-antithrombin complexes in patients with arterial and venous thrombosis. *Thromb Haemost* 2010;103(6):1188–92.
- [54] Zelaya H, Rothmeier AS, Ruf W. Tissue factor at the crossroad of coagulation and cell signaling. *J Thromb Haemost* 2018;16(10):1941–52.
- [55] Laszik Z, Mitro A, Taylor FB, Ferrell G, Esmon CT. Human protein C receptor is present primarily on endothelium of large blood vessels: implications for the control of the protein C pathway. *Circulation* 1997;96(10):3633–40.
- [56] Mammen EF. Disseminated intravascular coagulation (DIC). *Clin Lab Sci* 2000;13(4):239–45.
- [57] Bouck EG, Denorme F, Holle LA, et al. COVID-19 and sepsis are associated with different abnormalities in plasma procoagulant and fibrinolytic activity. *Arterioscler Thromb Vasc Biol* 2021;41(1):401–14.
- [58] Rovas A, Osiaevi I, Buscher K, et al. Microvascular dysfunction in COVID-19: the mystic study. *Angiogenesis* 2021;24(1):145–57.
- [59] Mancini I, Baronciani L, Artoni A, et al. The ADAMTS13-von willebrand factor axis in COVID-19 patients. *J Thromb Haemost* 2021;19(2):513–21.
- [60] Stanne TM, Pedersen A, Gisslen M, Jern C. Low admission protein C levels are a risk factor for disease worsening and mortality in hospitalized patients with COVID-19. *Thromb Res* 2021;204:13–5.
- [61] Dupont A, Rauch A, Staessens S, et al. Vascular endothelial damage in the pathogenesis of organ injury in severe COVID-19. *Arterioscler Thromb Vasc Biol* 2021;41(5):1760–73 ATVB/HA120315595.
- [62] Villa E, Critelli R, Lasagni S, et al. Dynamic angiopoietin-2 assessment predicts survival and chronic course in hospitalized patients with COVID-19. *Blood Adv* 2021;5(3):662–73.
- [63] Chioh FW, Fong SW, Young BE, et al. Convalescent COVID-19 patients are susceptible to endothelial dysfunction due to persistent immune activation. *Elife* 2021;10:e64909.
- [64] Jaffe EA. Cell biology of endothelial cells. *Hum Pathol* 1987;18(3):234–9.
- [65] Foley JH, Conway EM. Cross talk pathways between coagulation and inflammation. *Circ Res* 2016;118(9):1392–408.
- [66] Grover SP, Mackman N. Tissue factor: an essential mediator of hemostasis and trigger of thrombosis. *Arterioscler Thromb Vasc Biol* 2018;38(4):709–25.
- [67] Guervilly C, Bonifay A, Burtsey S, et al. Dissemination of extreme levels of extracellular vesicles: tissue factor activity in patients with severe COVID-19. *Blood Adv* 2021;5(3):628–34.
- [68] Rosell A, Havervall S, von Meijenfeldt F, et al. Patients with COVID-19 have elevated levels of circulating extracellular vesicle tissue factor activity that is associated with severity and mortality. *Arterioscler Thromb Vasc Biol* 2021;41(2):878–82.
- [69] Bain WG, Penalzoza HF, Ladinsky MS, et al. Lower respiratory tract myeloid cells harbor SARS-Cov-2 and display an inflammatory phenotype. *Chest* 2021;159(3):963–6.
- [70] Francischetti IM, Seydel KB, Monteiro RQ. Blood coagulation, inflammation, and malaria. *Microcirculation* 2008;15(2):81–107.
- [71] Liao M, Liu Y, Yuan J, et al. Single-cell landscape of bronchoalveolar immune cells in patients with COVID-19. *Nat Med* 2020;26(6):842–4.
- [72] Glas GJ, Van Der Sluys KF, Schultz MJ, Hofstra JJ, Van Der Poll T, Levi M. Bronchoalveolar hemostasis in lung injury and acute respiratory distress syndrome. *J Thromb Haemost* 2013;11(1):17–25.
- [73] Ruf W, Riewald M. Tissue factor-dependent coagulation protease signaling in acute lung injury. *Crit Care Med* 2003;31(4):S231–7 Suppl.
- [74] Antoniak S, Tatsumi K, Hisada Y, et al. Tissue factor deficiency increases alveolar hemorrhage and death in influenza a virus-infected mice. *J Thromb Haemost* 2016;14(6):1238–48.
- [75] Ma L, Shaver CM, Grove BS, et al. Kinetics of lung tissue factor expression and procoagulant activity in bleomycin induced acute lung injury. *Clin Transl Med* 2015;4(1):63.
- [76] Shaver CM, Grove BS, Putz ND, et al. Regulation of alveolar procoagulant activity and permeability in direct acute lung injury by lung epithelial tissue factor. *Am J Respir Cell Mol Biol* 2015;53(5):719–27.
- [77] Nossent EJ, Schuurman AR, Reijnders TDY, et al. Pulmonary procoagulant and innate immune responses in critically ill COVID-19 patients. *Front Immunol* 2021;12:664209.
- [78] Wolberg AS, Aleman MM, Leiderman K, Machlus KR. Procoagulant activity in hemostasis and thrombosis: virchow's triad revisited. *Anesth Analg* 2012;114(2):275–85.
- [79] Walters KA, D'Agostino F, Sheng ZM, et al. 1918 Pandemic influenza virus and streptococcus pneumoniae co-infection results in activation of coagulation and widespread pulmonary thrombosis in mice and humans. *J Pathol* 2016;238(1):85–97.
- [80] Calabretta E, Moraleda JM, Iacobelli M, et al. COVID-19-induced endotheliitis: emerging evidence and possible therapeutic strategies. *Br J Haematol* 2021;193(1):43–51.